MICROCRACKING IN CAST IRONS

G. Zambelli

Département des matériaux, Ecole Polytechnique Fédérale, Lausanne, Switzerland

ABSTRACT

The stages of microcracking of the graphite lamellae in eutectic oriented grey irons, with or without the addition of silicon, have been analysed by use of scanning electron microscopy (SEM). A special device giving rise to 4-point bending allows the observation of cracking in the lamellae at the surface under tension, as a function of measured strain. Cleavage cracking along the growth layers of the graphite occurs preferentially in the lamellae perpendicular to the tensile axis. There is no evidence of separation along the graphite-matrix interface. Correspondence has been established between the stages of microcracking of the lamellae and the pseudo-elastic, elasto-plastic and plastic deformation regions of grey cast iron. The importance of these regions depends on the size and shape of the graphite and the structure of the matrix both of which vary depending on the solidification speed and the absence or presence of silicon.

Key-words: eutectic grey cast iron, directional solidification, bending, scanning electron microscopy, rupture, graphite, cleavage, deformation regions.

INTRODUCTION

Grey cast iron is a material with a heterogeneous structure exhibiting essentially non-linear deformation (Angus, 1976). A study of the phenomenon of rupture makes it necessary to consider the role of graphite, as this component has a very limited capacity for withstanding loads and appears to be inextricably involved in crack initiation in grey iron.

During studies of rupture in grey irons, Clough and Shank observed separation of the graphite lamellae giving rise to voids on the surface of tensile specimens (Clough, 1957). Glover and Pollard confirmed this behaviour, noticing that the voids formed equally well at the centre as on the surface of the tensile specimens (Glover, 1971). These authors came to the conclusion that the separation of the lamellae and the initiation of cracks in the matrix, were the result of cleavage

rupture along the graphite's basal plane (0001). A different point of view of rupture in grey irons is put forward by Kuroda and Takada who have shown that crack initiation results from separation at the graphite-matrix interface (Kuroda, 1970). Prabhakar *et al.* have studied rupture in directionally solidified grey irons (Prabhakar, 1977). Here, rupture occurred by a combination of matrix-graphite separation and rupture at the boundaries of the crystallites making up the graphite lamellae. In effect, a lamella can be considered as an aggregate of tiny crystals of graphite (Lux 1957).

The present paper is limited to a study of the stages of microcracking in the graphite lamellae of directionally solidified eutectic grey cast irons with or without silicon addition. These grey irons have been produced by means of directional solidification starting from pure elements in order to govern the shape and size of the lamellae and to avoid the formation of eutectic cells.

The method chosen was one of observing, by means of scanning electron microscopy (SEM), the modes and stages of microcracking at the surface of microspecimens undergoing 4-point bending. Strain, as a function of gradual static loading, was measured by strain gauges fixed to the specimen surface. The results were compared with surface strains recorded by the same type of gauge fixed to tensile specimens. The idea of this correlation was to check the amount of strain of the microspecimen at the surface under tension, in comparison with the strain obtained during a normal tensile test.

EXPERIMENTAL

The grey irons chosen for this study were eutectic alloys - iron - 4.3 w/o carbon, and iron - 3.56 w/o carbon with 2.94 w/o silicon. These alloys were prepared from pure elements with sulphur and phosphorus levels at no more than 250 ppm and 150 ppm respectively.

The alloys were melted in alumina crucibles under an argon atmosphere, using induction heating, then poured into more alumina crucibles of dimensions 10x32x 150 mm. Directional solidification was brought about by lowering the crucible, at a measured speed, through a graphite resistance furnace (T = 1,450° C) with a cooled base giving rise to a temperature gradient of $G \sim 3 \times 10^4$ K m^{-1}. The Fe-C eutectic alloy was solidified at a speed of 3 cm h^{-1} (FE-3) and two Fe-C-Si eutectic alloys were solidified at speeds of 3 cm h^{-1} (FS-3) and 15 cm h^{-1} (FS-15).

Cylindrical tensile specimens 60 mm in length and 5 mm in diameter with threaded heads, and micro bend specimens 6x1x20 mm were machined parallel to the direction of solidification. An extensometer and a strain gauge fixed between the extensometers contact points along the tensile axis were used to measure the axial elongation of the tensile specimens. The measuring surface of the gauge was roughly 1 mm^2. The tensile tests were carried out on a mechanical testing rig (Zwick 1484) using a load of 100 kN and a constant draw speed of 0.1 mm/min. A special 4-point bending device (Fig. 1) was adapted for use in the specimen holder of the SEM (Cameca). Loading was carried out on an Instron 1127 apparatus (500N) and a threaded blocking system enabled the load to be held steady during observations. Load variations on holding, were checked by the strain gauge fixed on the tensile surface of the microspecimen under bending. The surface to be studied underwent

ionique bombarding for 90 h at an angle of 20°. This technique allows planar surfaces to be obtained, free of all residual stresses introduced by mechanical polishing. Further, this method allows one to expose the interface between the graphite lamellae and the matrix. In effect, using other methods of preparation of the surface to be studied, the interface is often obscured by the matrix.

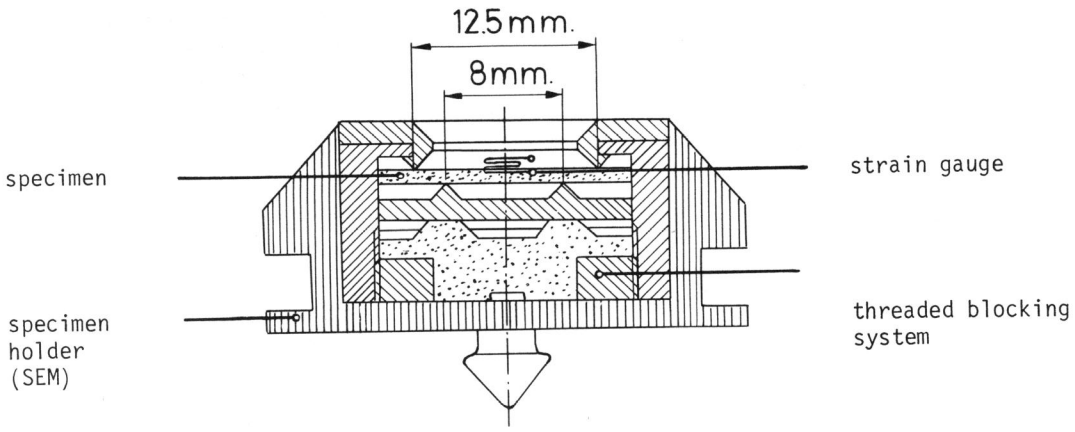

Fig. 1 Special 4-point bending device for microcracking observations in SEM

RESULTS

The microstructures of sections cut parallel to the direction of solidification of the grey irons under observation are shown in Fig. 2. The alloy FE-3 (Fig. 2a) is composed of a pearlite-ferrite matrix and a network of coarse graphite flakes of type A (ASTM, 1967). The matrix of alloy FS-3 (Fig. 2b) is ferritic Fe-Si with graphite lamellae of type A. The microstructure of alloy FS-15 (Fig. 2c) is composed of a ferritic Fe-Si matrix with a few fine dendrites oriented in the solidification axis, and of a fine, highly branched graphite network, comparable to a 'coral' structure (Lux, 1968). The high solidification speed gave rise to the formation of eutectic cells, probably due to the endogeneous character of solidification. The volume fraction, the dimensions and the shape of the graphite lamellae are different for the three alloys. Alloys FS-3 and FS-15 contain a ductile Fe-Si matrix whilst alloy FE-3 comprises a more brittle pearlite-ferrite matrix.

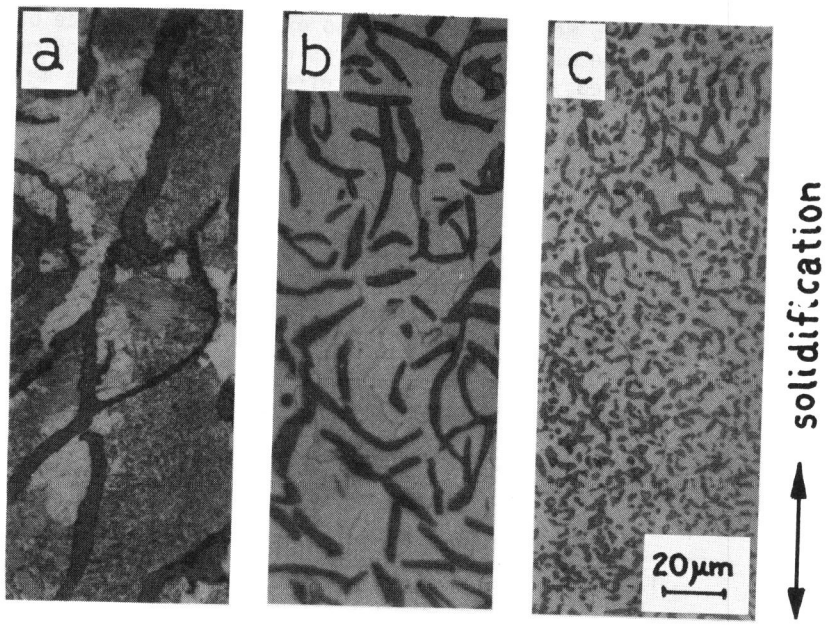

Fig. 2 Microstructures of grey irons. a) alloy FE-3, b) alloy FS-3, c) alloy FS-15. Etchant: Nital

The stress-strain, σ_{max} - ε_s, curves of the 4-point bend tests carried out on micro-specimens of the three types of grey irons are reported in Fig. 3. The maximum tensile stress σ_{max} at the external layers under flexion is calculated using the classical theory for the strength of materials. The measurement of surface strain εs is limited to $\varepsilon s \leq 0.7$ % due to loss of precision of gauge measurement. The stress-strain diagrams are not linear and permanent plastic strain is produced at low stresses (Gilbert 1957). Thus, the elasticity modulus diminishes with a growth in stress. This behaviour is particularly true for cast iron FE-3. For the FS series, the stress-strain diagrams exhibit a linear relationship up to a 'limit of proportionality'. This limit is higher when the graphite is finer (FS-15).

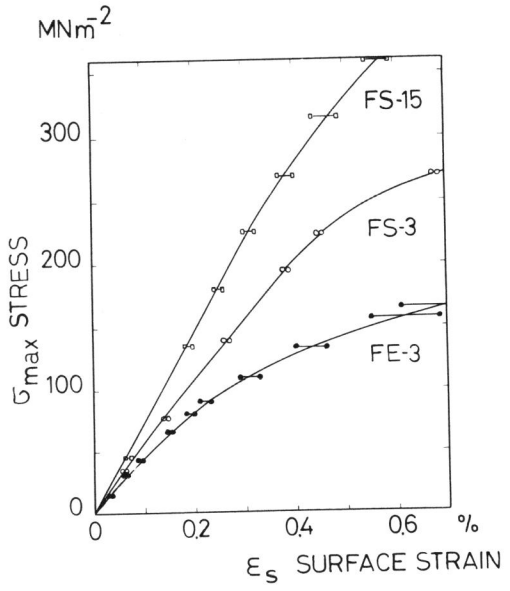

Fig. 3 Stress-strain curves of the 4-point bend tests of the grey irons

Fig. 4 shows a comparison of the stress-strain, σ-ε_S diagram for the tensile test with the bend test for grey iron Fe-3. Strain ε_S is that measured at the surface of the specimen under traction. The two curves can be superimposed during the initial elasto-plastic region only to diverge from $\varepsilon_S > 0.2$ %.

This behaviour is different for the FS grey irons as is shown by the tensile and bend curves for alloy FS-3, given in Fig. 5. From the outset, the tensile curve gives a strain ε_S, lower than that measured for the bend test, for the same calculated stress. This behaviour is reversed when the strain level rises above ε_S = 0.45 %. Identical behaviour is observed for the fine graphite alloy FS-15 but with a steeper slope at the start of the σ-ε_S curves and a higher stress level in the zone over which the tensile strain becomes greater than the bend strain - the reversal mentioned above. Once again, reversal occurs when the strain level rises above ε_S = 0.45 %. The tensile curves recorded using the extensometer are analogous to those obtained by use of the strain gauge. All the same, a systematic dropping off of strain towards lower levels, ε is observed. This behaviour can be attributed to delay in the measurements being registered, coupled to the poor sensitivity of the captor at the start of straining.

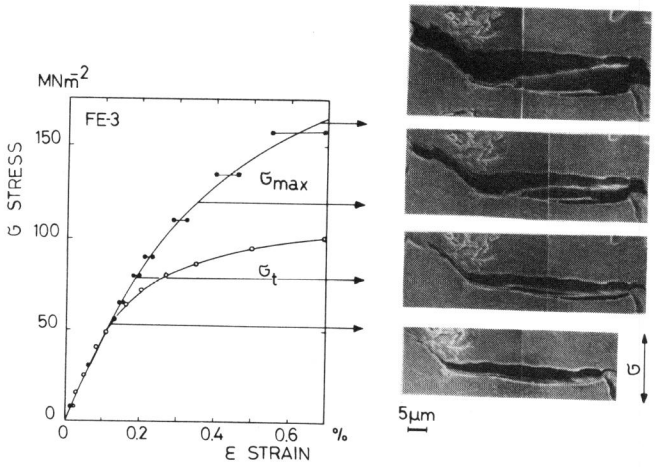

Fig. 4 σ_{max} - ε_s curve for the bend test and σ_t - ε_s curve for the tensile test for grey iron FE-3

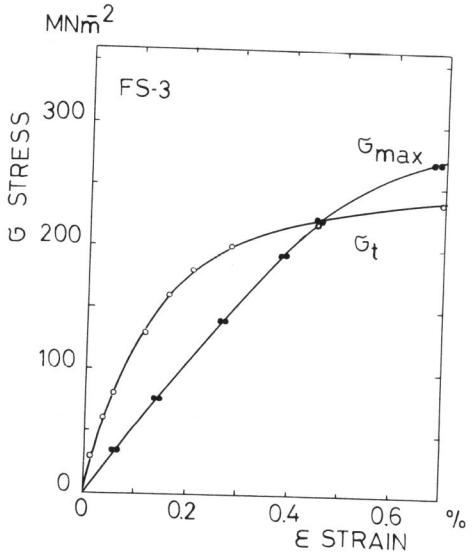

Fig. 5 σ_{max} - ε_s curve for the bend test and σ_t - ε_s curve for the tensile test for grey iron FS-3

The tensile strength of the grey irons are σ = 120 MNm^{-2} for alloy FE-3, σ = 260 MNm^{-2} for alloy FS-3 and σ = 350 MNm^{-2} for alloy FS-15. These values confirm results obtained from other studies using practically the same alloys and conditions (Prabhakar, 1977).

The stages of progressive microcracking in a lamella oriented perpendicularly to the tensile axis at the surface of a bend test (SEM) are illustrated by the photomicrographs in Fig. 4. The microcracks form near the interface and in the middle of the lamella surface, for a strain of ε_S = 0.12 %. The gradual opening of the microcracks takes place at strains greater than 0.12 %, together with a rise in the lamella's apparent surface (lamella + void).

A detailed examination of the start of microcracking of the graphite for ε_S = 0.12 % reveals failure by cleavage in the planes perpendicular to the lamellar surface, i.e. at right angles to the tensile axis (Fig. 6). The extension, in irregular steps, of cracking across the lamella can be attributed to preferential failure along the stratified graphite crystallite boundaries. The gradual opening of the microcracks (ε_S = 0.19 %, Fig. 7) confirms the formation of planar and irregular cleavage surfaces with sharply angled facets. The cleavages follow the limit of the graphite layers thus forming a network of planar symmetry slightly in relief. Tearing or discontinuous and irregular geometric relief patterns, typical of separation at the graphite-matrix interface, is not revealed.

With growth in deformation, a network of interconnected microcracks gradually forms perpendicular to the tensile axis. In the type of deformation studied, the graphite lamellae oriented parallel to the tensile axis suffer no cracking except at their extremities which are frequently curved.

General behaviour is observed for similar microcracking for grey irons FS-3 and FS-15. It should be noted, however, that there exists a critical strain ε_L which defines the first observation of microcracks in the lammellae. This limit corresponds to ε_L = 0.14 % for grey iron FS-3 and ε_L = 0.26 % for grey iron FS-15.

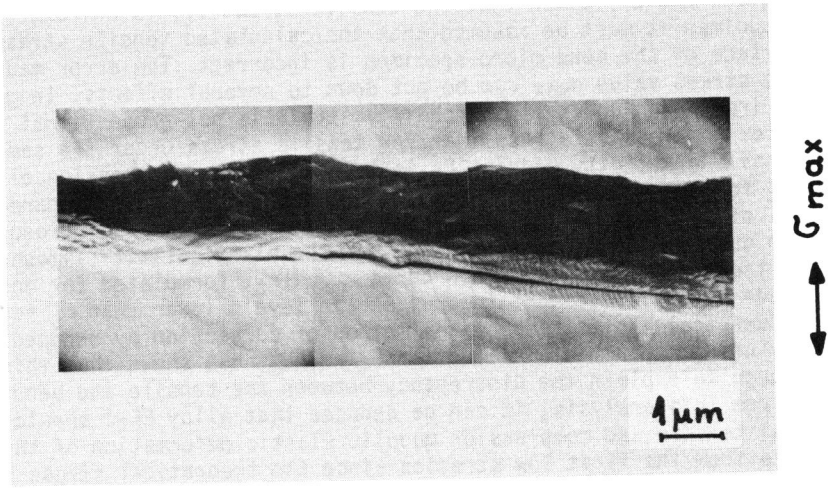

Fig. 6 Microcracking of the graphite for ε_S = 0.12 % for grey iron FE-3

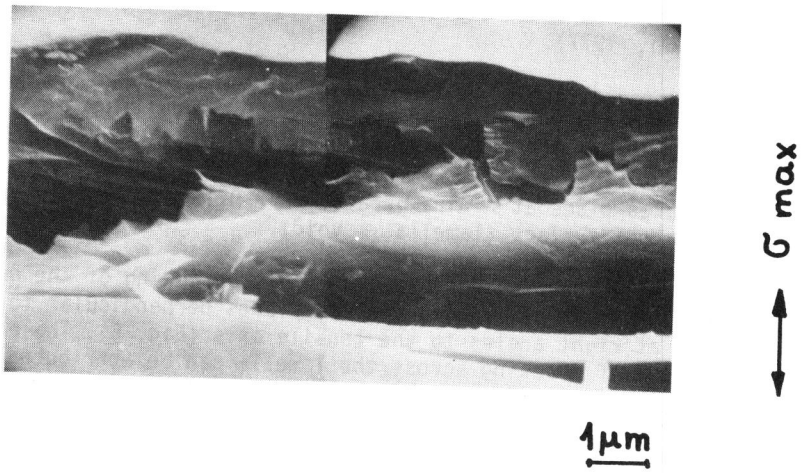

Fig. 7 Microcracking of the graphite for ε_s = 0.19 % for grey iron FE-3

DISCUSSION

For the same strain level ε_s, measured at the surface of the bend micro specimens and the tensile specimens, a discrepancy between the calculated stress values is noted (Figs. 4 and 5). Given that the tensile stress σ_t, is uniform over all the tensile specimen it must be assumed that the calculated tensile stress value σ_{max}, at the surface of the bend micro-specimen is incorrect. The error made in calculating the stress value σ_{max} can be put down to several effects. In general, for grey cast iron, even under light loading, strain is not proportional to charge and is lower for compressive stress than for tensile stress under the same values. As the tensile elasticity modulus E_t is lower than the compression elasticity modulus E_c for grey iron (Angus 1976) their behaviour can be compared to that of a material of 'reduced' elasticity modulus, E_r. This idea was introduced by Timoshenko during a study of strains beyond the elastic limit (Timoshenko 1968). The correction of the stress-strain curve σ_{max}- ε_s, formulated for modulus E_r, will be made by a displacement towards strain levels lower than ε_s for each $E_r > E_t$. Numerical application of the method of correction by reduced modulus of elasticity using experimental values of E_t and E_c, has shown that this correction is not enough to explain the discrepancy between the tensile and bend curves. However, from this analysis, it can be deduced that alloy FE-3 should have practically equal tensile and compression moduli. Plastic deformation of this grey iron takes place from the first low stresses since the theoretical stress σ_{max} becomes progressively greater than stress σ_t (Fig. 4). For the FS grey irons, plastic deformation would become noticeable beyond the yield point. Moreover, determination of real stress σ_{max} is made difficult due to the complex bending of the foil in

the SEM. The important contribution of shearing must be taken into consideration when calculating σ_{max}. Direct correlation between the tensile and bend tests must therefore be discounted when studying grey irons, thus confirming the results of Plénard (Plénard, 1967). For the analysis of the bending diagrams for the grey irons under study, it must be admitted that the calculated stress value σ_{max} is proportional to the real stress acting on the surface under traction. These bending diagrams can be described by three successive strain modes. A pseudo-elastic type of strain, recorded, in general, for very low stresses and limited by a proportional critical strain ε_L. This type can be defined by the simple relation:

$$\sigma_{max}/\varepsilon_s = E_o/K \qquad (1)$$

E_o is the elasticity modulus measured at the start of stressing and $K < 1$ is a correction factor. An elasto-plastic type follows that described above and is characterised by the following relation:

$$\sigma_{max}/\varepsilon_s = E/K(1-\alpha\sigma_{max}) \qquad (2)$$

where E is the mean modulus of elasticity different from modulus E_o. The constant α, depends at the same time on the morphology of the graphite and the elastic limit of the matrix. The last type of strain is characterised by overall plastic strain.

Expressing the bending diagrams in the form $\sigma_{max}/\varepsilon_s = f(\sigma_{max})$, curves are obtained, which allow an analysis of the stages of microcracking in grey cast irons (Fig. 8). The pseudo-elastic type was not revealed for eutectic grey iron FE-3, with coarse lamellar graphite and a pearlite-ferrite matrix. A relatively important elasto-plastic type was recorded. The value calculated for factor α, = 0.003, characterises the decisive role of the opening of microcracks in this type - opening favoured by the low strain energy capacity of the pearlite-ferrite matrix. The predominant action of plastic strain appears at stresses higher than σ_{max} = 140 MNm^{-2} (ε_c = 0.45 %).

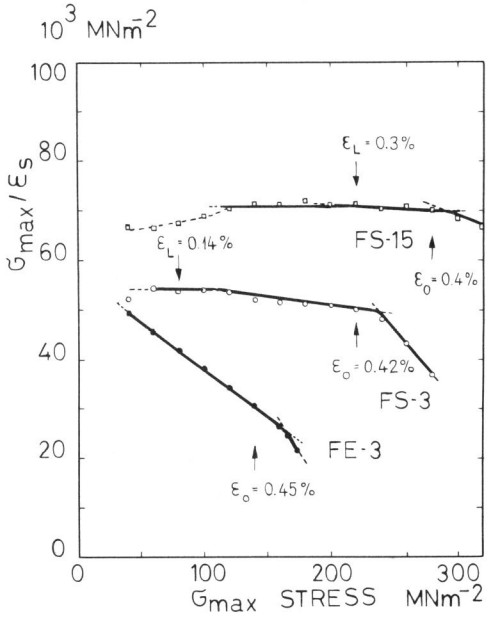

Fig. 8 $\sigma_{max}/\varepsilon_s - \sigma_{max}$ curves for grey cast irons

The introduction of silicon into eutectic grey cast iron, for a given solidification speed (FS-3), gives rise to the formation of a network of finer graphite in a ductile Fe-Si matrix. Pseudo-elastic type of behaviour is apparent up to stress level σ_{max} = 100 MNm^{-2} (ε_L = 0.14 %) followed by elasto-plastic behaviour characterised by a very low α factor (α = 0.0005). This behaviour indicates that the action of microcracking and of the opening of the graphite lamellae, diminishes due to the greater capacity of the Fe-Si matrix to absorb elastic energy. General plastic strain capacity for this grey iron appears at stresses greater than 220 MNm^{-2} (ε_o = 0.42 %). The overall behaviour of alloy FS-3 is also observed for alloy FS-15 at a greater solidification speed. The microstructure composed of fine graphite in a Fe-Si matrix promotes the existence of a pseudo-elastic region which is evident up to stress level σ_{max} = 220 MNm^{-2} (ε_L = 0.30 %). The elasto-plastic region becomes shorter and poorly defined. Factor α, however, remains very small. Plastic strain appears for stresses greater than 280 MNm^{-2} (ε_o = 0.40 %). Nevertheless this limit can be equaly attributed to ε_L, limit of pseudo-elastic behaviour.

It is possible to establish correspondence between the stages of micro-cracking observed in graphite lamellae perpendicular to the tensile axis and the limits ε_L and ε_o of the strain regions. For eutectic grey iron FE-3, the absence of a pseudo-elastic region (indefinite ε_L) corresponds to the discovery of micro-cracking of the lamellae at the onset of low stressing. The extension of the voids created by the gradual separation of the lamellae, constitutes the general mechanism of elasto-plastic behaviour. For silicon-grey irons FS-3 and FS-15, observation of the micro-cracks (limited by the resolving power of the SEM) coincides with the end of the pseudo-elastic region, defined by the proportionality limit ε_L. This inaccuracy in the critical limit in the case of alloy FS-15 can be put down to the presence of a type of graphite of different morphology. Further, the diminution of distance between the lamellae can modify stress relaxing conditions in the Fe-Si matrix.

The start of the predominant effect of plastic strain in the failure process of the three grey irons under study, seems to be connected with a critical opening of microcracks, proportional to the lamellae thickness or to the inter-lamellae spacing. In effect, the value which defines the start of plastic strain, is practically constant for the three grey irons at $\varepsilon_o \simeq 0.40$ %

This study of the stages of graphite cracking in grey cast irons is of a preliminary nature. Not taken into account are the surface distribution of the lamellae and the correlation between the state of microcracking at the surface and that in the bulk of the metal.

CONCLUSIONS

Micro-cracking in orientated eutectic grey cast irons, with or without the addition of silicon, is dependent on the parameters of the graphite network and on the structure of the matrix. Propagation of the graphite's microcracks takes place solely by multiple cleavage within the lamellae perpendicular to the tensile axis, without obvious interface separation. The gradual opening of the cracks during the deformation stages leads to elasto-plastic strain in grey irons. This formation of voids by separation of the lamellae is greater for coarse graphite in eutectic grey irons without silicon. A region of pseudo-elastic strain, without visible cracking

of the graphite, is apparent for grey irons with silicon additions. This behaviour can be attributed to the action of the change of shape and size of the graphite lamellae and to the greater strain energy of the Fe-Si matrix. The start of the plastic strain region corresponds to a surface strain value practically identical for each grey cast iron studied. The real stress acting at the surface of the bend test cannot be compared with that measured at the surface of the tensile test. A bend test carried out on micro-specimens gives rise therefore, to a condition of complex stresses which should be better defined but which corresponds to working conditions met in grey irons, characterised by a lack of proportionality of working strains.

ACKNOWLEDGEMENTS

We would like to thank B. Senior of the Institut Inderdépartemental de Métallurgie (Swiss Federal Institute of Technology, Lausanne) and Y. Neuenschwander for their close collaboration during this work. This study was supported by the Fonds National Suisse de la Recherche Scientifique - national research programme: matières premières et matériaux.

REFERENCES

Angus, H.T. (1976). Cast iron, Butterwoths, second edition
ASTM A 247-67 (1967). Standard Method for Evaluating the Microstructure of Graphite in Iron Castings
Clough W.R., Shank M.F. (1957). Trans. ASM, 49, 241-262
Gilbert G.N.J. (1957). Brit. Cast Iron Res. and Dev. 6, 546
Glover A.G., Pollard G. (1971). J. Iron Steel Inst., 138-141
Kuroda Y., Takada H. (1970). ASF Cast Metals Res. J., 63-74
Lux B., Grages M. (1968). Prakt. Metall. 5, 123-126
Lux B., Bollmann W., Grages M. (1969). Practical Metallography 6, 530
Plénard E., Bontault J., Gatélier P. (1967). Fonderie, 260, 363-375
Prabhakar K.V., Nieswaag H., Zwithoff A.J. (1977). Solidification and Casting of Metals. Proc., 444-453
Timoshenko S. (1968). Résistance des matériaux. Dunod tome 2.